Inorganic Chemistry

Article

pubs.acs.org/IC

B–H Bond Activation Using an Electrophilic Metal Complex: Insights into the Reaction Pathway

Rahul Kumar and Balaji R. Jagirdar*

Department of Inorganic & Physical Chemistry, Indian Institute of Science, Bangalore 560012, India

Supporting Information

ABSTRACT: A highly electrophilic ruthenium center in the $[RuCl(dppe)_2][OTf]$ complex brings about the activation of the B–H bond in ammonia borane ($H_3N{\cdot}BH_3$, AB) and dimethylamine borane ($Me_2HN{\cdot}BH_3$, DMAB). At room temperature, the reaction between $[RuCl(dppe)_2][OTf]$ and AB or DMAB results in *trans*-$[RuH(\eta^2\text{-}H_2)(dppe)_2][OTf]$, *trans*-$[RuCl(\eta^2\text{-}H_2)(dppe)_2][OTf]$, and *trans*-$[RuH(Cl)(dppe)_2]$, as noted in the NMR spectra. Mixing the ruthenium complex and AB or DMAB at low temperature (198/193 K) followed by NMR spectral measurements as the reaction mixture was warmed up to room temperature allowed the observation of various species formed enroute to the final products that were obtained at room temperature. On the basis of the variable-temperature multinuclear NMR spectroscopic studies of these two reactions, the mechanistic insights for B–H bond activation were obtained. In both cases, the reaction proceeds via an η^1-B–H moiety bound to the metal center. The detailed mechanistic pathways of these two reactions as studied by NMR spectroscopy are described.

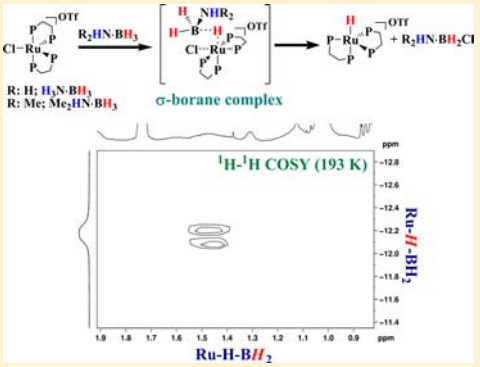

INTRODUCTION

The activation of the very inert C–H bond in simple alkanes, e.g., CH_4, C_2H_6, cyclohexane, etc., and its subsequent functionalization using transition-metal complexes have remained challenging problems since the late 1950s.[1] The weak nature of the M–H–C interaction makes it very difficult to study the binding and activation of the C–H bonds in alkanes under ambient conditions. The binding and cleavage of the X–H (X = H, Si, B) bonds of other molecules such as dihydrogen, silanes, and borane–Lewis base adducts have close resemblances with one another and are quite significant because they serve as models for the activation and functionalization of the C–H bond in methane and other alkanes. Whereas a large number of the so-called σ complexes bearing H_2 and Si–H[2−6] as a ligand/ligand fragment have been reported, the synthesis and characterization of coordination compounds with saturated hydrocarbons as ligands have been particularly challenging.[7−10] On the other hand, four-coordinated boranes are isoelectronic with methane; the B–H bond in these species binds with metal centers in a stable M–H–B interaction and could serve as good models for the C–H binding and activation.

Hartwig et al. demonstrated the η^2 binding of a three-coordinated borane, which paved the way to exploration of the coordination chemistry of three-coordinated borane complexes.[11] On the other hand, the chemistry of the four-coordinated boron species has been undergoing rapid development with the introduction of the Lewis base–borane complexes of the $M(CO)_5$ (M = Cr, Mo, W) fragment by Shimoi et al.[12] In this context, ammonia borane has been the focus of recent research interest not only from the standpoint of the B–H binding to the metal center and its subsequent activation but also from its potential as a hydrogen source and storage material.[13,14] Although several systems are known to bring about dehydrogenation of ammonia borane and the substituted amine boranes the intricate mechanisms of these reactions involving the B–H bond activation and the ability of the metal complexes to retain a B–N moiety in the reaction sequence are yet to be fully elucidated.[13,14] Recently, Alcaraz and Sabo-Etienne reviewed the progress made in the coordination chemistry of ammonia borane and the substituted amine boranes.[13] In addition, reports on σ complexes of amine boranes, coordinated aminoborane to the metal center, and ammonia borane dehydrogenation using transition-metal catalysts have also appeared.[15] In our effort to study the binding and activation of the B–H bond to electrophilic metal centers, we recently undertook the task of studying the reactivity of ammonia borane and the related amine boranes toward the five-coordinated ruthenium complex $[RuCl(dppe)_2][OTf]$ [**1**; dppe = 1,2-bis(diphenylphosphino)ethane, $Ph_2PCH_2CH_2PPh_2$; OTf = $CF_3SO_3^-$]. Herein, we describe the results of the mechanistic studies of those reactions.

EXPERIMENTAL SECTION

General Procedures. All manipulations were carried out under a dry and oxygen-free N_2 atmosphere using standard Schlenk and inert-atmosphere techniques unless otherwise specified. Reagent-grade solvents were dried and distilled under a N_2 atmosphere from sodium benzophenone [hexane, petroleum ether, tetrahydrofuran (THF),

Received: February 21, 2012
Published: December 17, 2012

   dx.doi.org/10.1021/ic300390s | *Inorg. Chem.* 2013, 52, 28−36

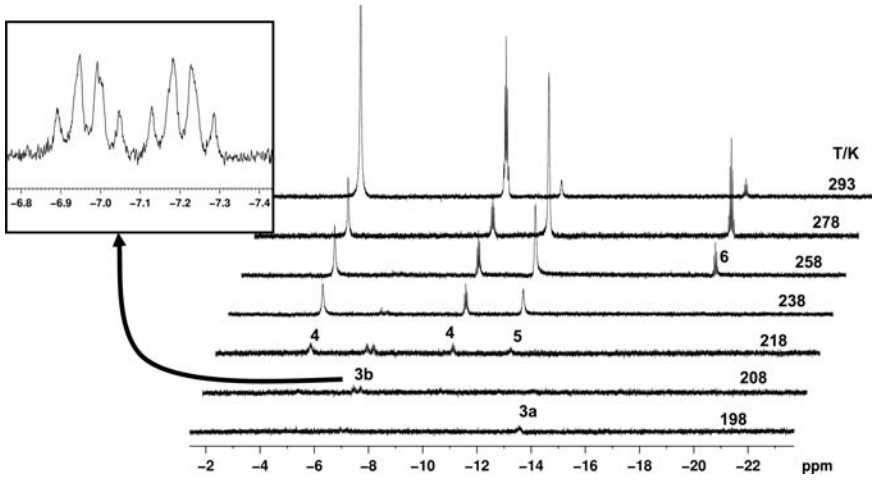

Figure 1. ^{1}H NMR spectral stack plot with temperature showing intermediates **3a** and **3b** and complexes **4**−**6** in the reaction of complex **1** with AB in CD_2Cl_2.

diethyl ether] just before use. Dichloromethane was first dried and distilled using P_2O_5 and then dried and distilled over CaH_2. Dichloromethane-d_2 (CD_2Cl_2) was purchased from Cambridge Isotope Ltd., USA, and used as received. Methanol was dried and distilled using MgI_2, whereas acetone was dried and distilled over K_2CO_3.

Ammonia borane ($H_3N{\cdot}BH_3$, AB) and $H_3N{\cdot}BD_3$ (ABD) were synthesized according to literature procedures.[16] The amine borane adduct, dimethylamine borane ($Me_2HN{\cdot}BH_3$, DMAB), was purchased from Sigma-Aldrich and was purified by sublimation prior to use. The [RuCl(dppe)$_2$][OTf] complex **1** was prepared using the reported method.[17]

The ^{1}H, $^{31}P\{^{1}H\}$, ^{11}B, and ^{19}F NMR spectral data were obtained using an Avance Bruker 400 MHz instrument. The $^{31}P\{^{1}H\}$ NMR spectra were recorded relative to 85% H_3PO_4 (aqueous solution) as an external standard and the ^{19}F NMR spectra relative to $CFCl_3$. Variable-temperature (VT) NMR experiments were carried out in flame-sealed (in vacuo) NMR tubes. The ^{1}H and ^{31}P spin−lattice relaxation time (T_1) measurements were carried out using the inversion−recovery method.[18]

Reaction of Complex 1 with $H_3N{\cdot}BH_3$, AB (1:1). In a thoroughly dried Schlenk NMR tube having a Teflon stopcock, complex **1** (22 mg, 0.02 mmol) and AB (0.7 mg, 0.02 mmol) were loaded and the tube was evacuated and then refilled with N_2 gas. It was then immersed in a liquid N_2 bath, and CD_2Cl_2 (0.7 mL) was added quickly under a positive flow of N_2 gas such that the solvent froze before coming into contact with the solid components at the bottom of the tube. The stopcock was quickly replaced, and the tube was once again evacuated and held under vacuum for about 20−30 min with the contents in the frozen state. The stopcock was closed tightly, and the tube was flame-sealed with the contents still in the frozen state. It was then inserted into the NMR probe, which was precooled to 198 K, and the ^{1}H, $^{31}P\{^{1}H\}$, and ^{11}B NMR spectra were recorded. The reaction progressed as the temperature was raised. Figures 1 and 2 show the VT ^{1}H and $^{31}P\{^{1}H\}$ NMR spectral stack plots, respectively, of this reaction. The same reaction was also carried out at room temperature, and the products were characterized using NMR spectroscopy. The relative percentages of the products obtained in this reaction at room temperature are summarized in Table 1. The NMR spectra have been deposited in the Supporting Information. At room temperature, the intense-dark red-colored solution of the reaction mixture turned pale yellow instantaneously accompanied by vigorous gas evolution, which ceased after a few minutes, and an off-white-colored precipitate also formed.

Reaction of Complex 1 with $Me_2HN{\cdot}BH_3$, DMAB (1:1). This reaction was conducted in a manner similar to that of complex **1** with AB starting with 22 mg (0.02 mmol) of complex **1** and 1.3 mg (0.02 mmol) of DMAB. The sealed NMR tube with the frozen contents was

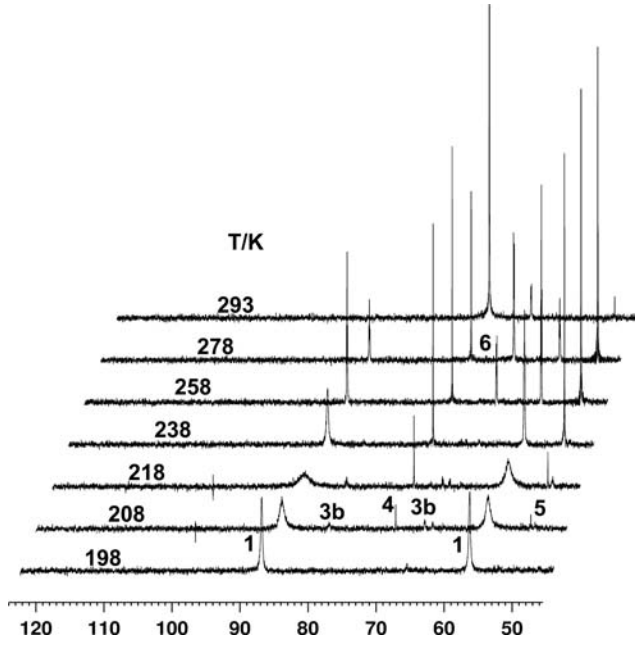

Figure 2. $^{31}P\{^{1}H\}$ NMR spectral stack plot with temperature showing intermediate **3b** and complexes **4**−**6** in the reaction of complex **1** with AB in CD_2Cl_2.

Table 1. Relative Percentage of Complexes 4−6 after the Reaction of Complex 1 with AB and DMAB at 298 K[a] in Stoichiometric Ratio 1:1

reagent	4	5	6
AB	96	trace	4
DMAB	44	28	28

[a]Integrations of the peaks were done after ensuring that no further change in the peak intensities took place, which signaled that the reaction had gone to completion.

inserted into the NMR probe precooled to 193 K, and the ^{1}H, $^{31}P\{^{1}H\}$, and ^{11}B NMR spectra were recorded as the reaction progressed upon an increase in the temperature. Figures 3−5 show the ^{1}H NMR spectral stack plot, ^{1}H−^{1}H COSY spectrum, and $^{31}P\{^{1}H\}$ NMR spectral stack plot, respectively, of this reaction. The same reaction was carried out at room temperature, and in this case as well, the products were identical with those of the reaction of complex **1**

dx.doi.org/10.1021/ic300390s | Inorg. Chem. 2013, 52, 28−36

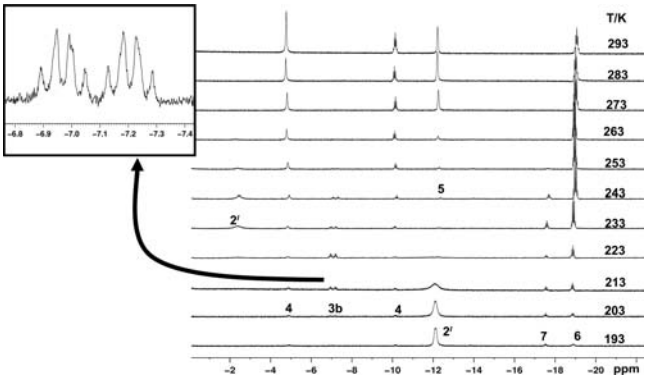

Figure 3. ^{1}H NMR spectral stack plot showing intermediates **2′** and **3b** and complexes **4**–**7** in the reaction of complex **1** with DMAB in CD_2Cl_2.

with AB. The relative percentages of the products obtained in this reaction are summarized in Table 1.

Reaction of Complex 1 with $H_3N{\cdot}BD_3$ (1:1). In a 5 mm NMR tube, complex **1** (11 mg, 0.01 mmol) and $H_3N{\cdot}BD_3$ (0.4 mg, 0.01 mmol) were loaded, and the tube was capped with a septum. Then CD_2Cl_2 (0.7 mL) was added under a flow of N_2 gas, and the ^{1}H NMR spectrum of the reaction mixture was recorded immediately upon mixing the contents of the tube to observe the formation of isotopomers (spectra have been deposited in the Supporting Information).

Reaction of Complex 1 with Excess AB and DMAB. These reactions were carried out in a manner similar to that of complex **1** with AB and DMAB (1:1 stoichiometric amounts). Complex **1** (11 mg, 0.01 mmol) was treated with AB (3.2 mg, 0.1 mmol) and DMAB (6.0 mg, 0.1 mmol) in separate NMR tubes in a CD_2Cl_2 solvent. The sealed NMR tube with the frozen contents was inserted into the NMR probe precooled to 193 K, and the ^{1}H, ^{31}P{^{1}H}, and ^{11}B NMR spectra were recorded as the reaction progressed upon an increase in the temperature. The ^{1}H, ^{31}P{^{1}H}, and ^{11}B NMR spectral stack plots are given in Supporting Information. The same reactions were carried out at room temperature as well (for spectra, see the Supporting Information).

Reaction of DMAB with HOTf (1:1): Characterization of $Me_2HN{\cdot}BH_2(OTf)$. In a regular NMR tube, DMAB (6 mg, 0.1 mmol) was dissolved in 0.4 mL of dried and degassed dichloromethane and then HOTf (9 μL, 0.1 mmol) was added followed by another 0.2 mL of CH_2Cl_2. Vigorous bubbling was noted. The ^{11}B NMR spectrum was recorded immediately after the reaction, which shows $Me_2HN{\cdot}BH_2(OTf)$ formation along with a small amount of unreacted DMAB (see the Supporting Information).

Synthesis of *trans*-[Ru(H)(NH_3)(dppe)$_2$][OTf] and Its Characterization by NMR Spectroscopy. A reaction mixture of complexes **4**–**6** and *trans*-[Ru(H)(NH_3)(dppe)$_2$][OTf] (from the reaction of complex **1** with AB) was added to 50–60 mL of ammoniacal dichloromethane (CH_2Cl_2 dissolved in liquid ammonia, 243 K) in a Schlenk flask and stirred for ∼30 min. Then, the volume was reduced to 10 mL. After that, ∼15 mL of hexane was added, which resulted in the formation of an off-white precipitate. It was washed several times with hexane and dissolved in dichloromethane, and the ^{1}H and ^{31}P{^{1}H} NMR spectra were recorded (see the Supporting Information for the spectra).

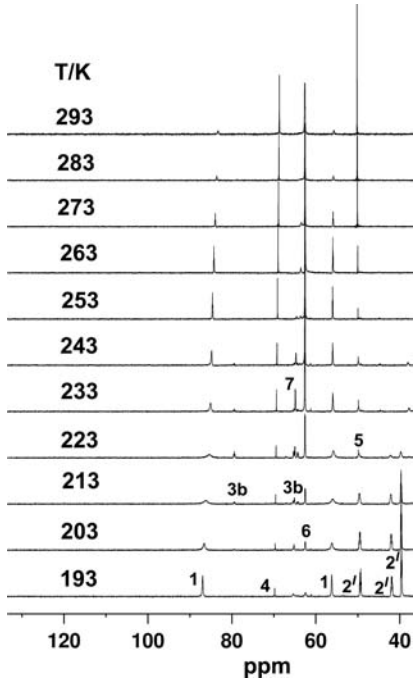

Figure 5. ^{31}P{^{1}H} NMR spectral stack plot with temperature showing intermediates **2′** and **3b** and complexes **4**–**7** in the reaction of complex **1** with DMAB in CD_2Cl_2.

RESULTS AND DISCUSSION

Reaction of Complex 1 with AB (1:1). The [RuCl(dppe)$_2$][PF_6] complex was reported by Morris and his coworkers.[19] In spite of being a coordinatively unsaturated 16-electron species, it is air-stable in solution and reacts with small molecules such as H_2, CO, and CH_3CN to afford the respective 18-electron derivatives. This compound also brings about the catalytic hydrogenation of trimethylsilyl enol ethers to cyclohexanone and Me_3SiH.[20] The reaction involves heterolytic cleavage of the bound H_2 ligand as a key step, wherein a H^+ is transferred to the O atom of the enol ether. We chose to use

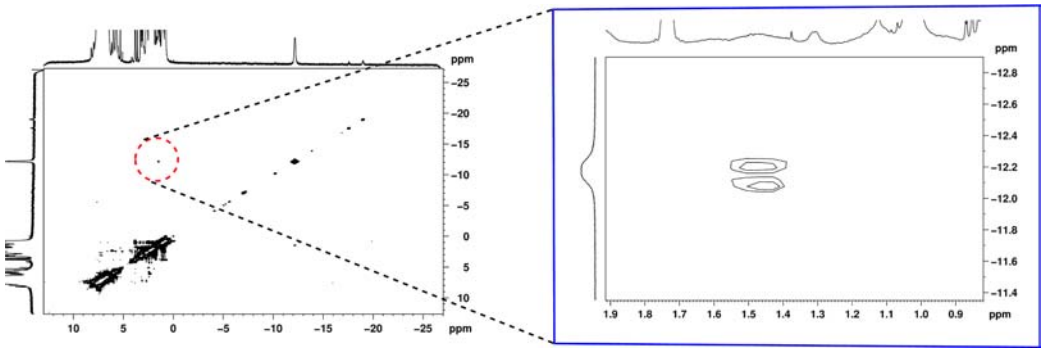

Figure 4. ^{1}H–^{1}H COSY spectrum showing the off-diagonal cross peak for the σ-borane intermediate (**2′**) in the reaction of complex **1** with DMAB at 193 K in CD_2Cl_2. Figure at the right after zooming.

dx.doi.org/10.1021/ic300390s | *Inorg. Chem.* 2013, 52, 28–36

[RuCl(dppe)$_2$][OTf] to explore its reactivity with AB and DMAB (Scheme 1). AB and DMAB are simple Lewis acid−base adducts in which the BH H atoms are hydridic and the NH H atoms are acidic in nature. The reaction of **1** with AB or DMAB at room temperature resulted in the formation of *trans*-[RuH(η^2-H$_2$)(dppe)$_2$][OTf] (**4**), *trans*-[RuCl(η^2-H$_2$)(dppe)$_2$]-[OTf] (**5**), and *trans*-[RuH(Cl)(dppe)$_2$] (**6**) complexes and $H_3N{\cdot}BH_2Cl$[21] or $Me_2HN{\cdot}BH_2Cl$,[22] as evidenced by NMR spectroscopy (Scheme 1; see the Supporting Information for spectra).

Scheme 1. Reaction of Complex 1 with Amine Boranes

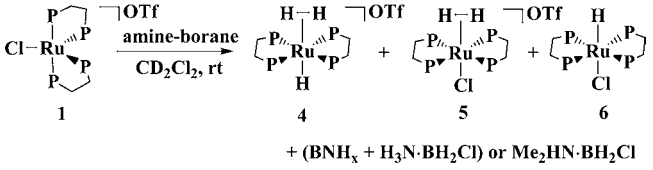

The spectral properties of **4**−**6** matched those of the reported ones.[19,23] The relative percentages of **4**−**6** formed in these reactions are summarized in Table 1. Although AB is not completely soluble in CD_2Cl_2, yet it reacts vigorously with [RuCl(dppe)$_2$][OTf] accompanied by H_2 gas evolution. The dark red solution of **1** in CD_2Cl_2 instantaneously faded to pale yellow, and an off-white precipitate also formed. Because the NMR spectra showed the presence of only B−H bond-cleaved products and no intermediate species, it suggests that the reaction proceeds very rapidly at room temperature.

Therefore, we carried out the same reaction at low temperature and monitored the progress of the reaction using VT NMR spectroscopy in order to gain insight into the mechanistic aspects. The VT ^{1}H and ^{31}P{^{1}H} NMR spectral stack plots of this reaction are shown in Figures 1 and 2, respectively, and the proposed mechanism is given in Scheme 2.

Complex **1** adopts a trigonal-bipyramidal geometry in solution and is stable in CH_2Cl_2 for several days. An electron-rich ligand could approach the metal center trans to the Cl and in between the two equatorial P atoms, resulting in a six-coordinated species having a trans geometry. A second possibility could also be considered, wherein a B−H bond will approach the Ru center trans to one of the equatorial P atoms and adjacent to the Cl atom. These two possibilities result in the intermediate species **2a** and **2b** (unobserved; see Scheme 2). These unobserved intermediates undergo rapid B−H bond cleavage reactions. In the case of intermediate **2a**, the $[H_3N{\cdot}BH_2]^+$ species that results upon B−H bond cleavage abstracts the Cl^-. On the other hand, intermediate **2b** undergoes B−H and Ru−Cl metathesis. In both the cases (Scheme 2, step ii), $H_3N{\cdot}BH_2Cl$ is eliminated. Elimination of $H_3N{\cdot}BH_2Cl$ from the intermediate **2a** results in a five-coordinated species, [RuH(dppe)$_2$][OTf] (**3a**), adopting a square-pyramidal geometry. The quintet pattern [J(H,P$_{cis}$) = 18.0 Hz] at δ −13.9 ppm in the ^{1}H NMR spectrum is consistent with the square-pyramidal geometry of species **3a**. This species appears at 198 K. The metathesis reaction results in the formation of yet another five-coordinated species, [RuH(dppe)$_2$][OTf] (**3b**), adopting a trigonal-bipyramidal geometry. The species **3b** exhibits a doublet of a quartet at δ −7.1 ppm in the ^{1}H NMR spectrum at a temperature (208 K) higher than that of **3a**. The doublet pattern is due to trans H−P coupling on the order of 95.4 Hz, and the quartet [J(H,P$_{cis}$) = 20.6 Hz] results from the coupling of the hydride H atom with the three *cis*-P atoms. Perutz and his co-workers reported a quintet pattern at δ −11.9 ppm [J(H,P$_{cis}$) = 20.0 Hz] and a singlet at δ 52.6 ppm in the ^{1}H and ^{31}P{^{1}H} NMR spectra, respectively, in THF-d_8 for complex **3a**.[24] Complex **3b** is hitherto unknown. As the temperature of the reaction mixture is raised, **3a** undergoes isomerization to **3b** (Scheme 2, step iii), which is evident from the disappearance of the ^{1}H NMR spectral signal of **3a** and the increase in the signal intensity of **3b** at 208 K (Figure 1). This is a minor pathway by which **3b** is produced in addition to the main route via the metathetical reaction in **2b**. The B−H bond cleavage product, $H_3N{\cdot}BH_2Cl$, was noted in the ^{11}B NMR spectrum as a triplet at δ −9.0 ppm (see the Supporting Information).[21] On the basis of the prior

Scheme 2. Proposed Mechanism of the Reaction of Complex 1 with AB[a]

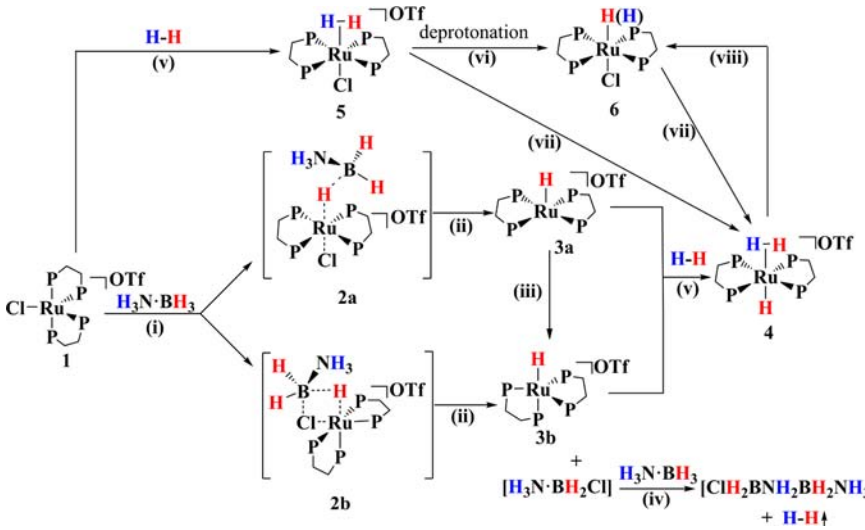

[a]Step vii: transformation of **5** or **6** to **4** takes place in the presence of **6** or **5**, respectively Step viii: transformation of **4** to **6** takes place in the presence of Cl^-.

dx.doi.org/10.1021/ic300390s | Inorg. Chem. 2013, 52, 28−36

theoretical work of Baker et al.,[25,26] we propose that this species reacts with unreacted AB, resulting in the dehydrogenation of AB in sequential fashion, and leads to formation of the BNH_x polymer via an unobserved oligomeric species $[BH_2ClNH_2BH_2NH_3]$. We also cannot rule out other pathways for the dehydrogenation of AB such as concerted B−H and N−H activation[15t] or stepwise B−H and N−H activation at the metal center.[15g] The H_2 generated via these reactions has two possible substrates to react with: (i) reaction with **3a** and **3b** to afford **4** and (ii) reaction with the starting complex $[RuCl(dppe)_2][OTf]$, resulting in the corresponding dihydrogen complex **5** (see Scheme 2, step v). We noted the formation of both **4** and **5** at 218 K (Figures 1 and 2 and Scheme 2). Complexes similar to **4** and **5** with BPh_4^- and PF_6^- counterions, respectively, were reported by Morris et al.[19,23] Complex **4** shows a quintet at δ −10.5 ppm (Ru−*H*) and a broad singlet at δ −4.8 ppm (Ru−η^2-H_2) in the ^1H NMR spectrum and a sharp singlet at δ 68.0 ppm in the $^{31}P\{^1H\}$ NMR spectrum; on the other hand, complex **5** shows a broad singlet at δ −12.3 ppm in the ^1H NMR and a sharp singlet at δ 51.5 ppm in the $^{31}P\{^1H\}$ NMR spectra.[19,23] Upon warming of the reaction mixture further, the concentrations of **4** and **5** increased, as was evident from an increase in their signal intensities in the ^1H NMR spectra (Figure 1). It is interesting to note that a singlet appears transiently at δ 4.6 ppm in the ^1H NMR spectrum, which could be ascribed to free H_2 before it reacts with the respective substrates. Whereas compound **4** persists upon warming the reaction mixture to room temperature, the bound H_2 in compound **5** undergoes heterolysis to afford the hydride derivative **6** (Scheme 2, step vi). Heterolysis of the bound H_2 in **5** in the presence of a base leads to the formation of **6**, which shows a quintet at δ −18.9 ppm in the ^1H NMR spectrum and a sharp singlet at δ 62.3 ppm in the $^{31}P\{^1H\}$ NMR spectrum. The spectral stack plots (Figures 1 and 2) suggest that complexes **5** and **6** transform into complex **4** to a certain extent; however, the pathway that they take is not clear. This was reported earlier by Morris and co-workers.[19] Complex **4** in the presence of Cl^- ion could transform into complex **6**, as reported by Morris and co-workers;[19] it is not clear whether the same is happening in our case because there is another Cl^- acceptor in the reaction solution, namely, $[H_3N{\cdot}BH_2]^+$. On the basis of $^{31}P\{^1H\}$ inversion−recovery and spin-saturation transfer experiments on the reaction mixture, we noted that the transformation of **5** or **6** to **4** takes place in the presence of **6** or **5**, respectively, with slow reaction rates (Scheme 2, step vii, and the Supporting Information). Additionally, we independently established the transformation of **4** to **6** in the presence of Cl^- ion and also the transformation of **5** and **6** to **4** (see the Supporting Information). Thus, complexes **4** and **6** undergo interconversion through different pathways. The interconversion of **6** and **4** becomes facile with an increase in the temperature, which leads to the expected gradual drop in the ^{31}P T_1 values. However, we observed ^{31}P T_1(min) at 263 K for **4** and **6** (see the Supporting Information), which suggests their slower interconversion and tumbling rate below 263 K and faster above it in comparison to their respective Larmor frequencies.[27] The appearance of **4**−**6** upon warming of the sample in this experiment to room temperature in the ^1H NMR spectrum is consistent with the observations made in the room temperature NMR spectral data. The spectral changes observed in the ^1H NMR spectra with temperature matched those of the $^{31}P\{^1H\}$ NMR spectral data shown in Figure 2.

The peaks corresponding to **1** broaden and then resharpen as the temperature is increased. Mezzetti et al. studied the dynamic behavior of an analogous species, $[RuCl(dcpe)_2][BPh_4]$ [dcpe = 1,2-bis(dicyclohexyl)phosphinoethane, $(C_6H_{11})_2PCH_2CH_2P(C_6H_{11})_2$].[28] Our observations with regard to VT NMR spectral behavior for complex **1** were similar to those of the $[RuCl(dcpe)_2][BPh_4]$ complex. Mezzetti et al. did not elaborate on these observations. We propose that the observed low-temperature NMR spectral behavior of complex **1** could be attributed to the stereochemical rigidity resulting from a favored weak interaction in a position cis to chloride (in an octahedral geometry) of triflate (OTf) counterion or the ortho protons of the phenyl group of the dppe ligand with the metal center (see the VT ^1H, ^{31}P, and ^{19}F NMR spectral stack plots in the Supporting Information). We noted broadening and an upfield shifting of one of the phenyl proton signals in the ^1H NMR spectra, broadening and downfield shifting of the ^{31}P NMR spectral signals, and upfield shifting of the ^{19}F NMR spectral signal at low temperatures (233−223 K). These observations suggest that the ortho protons of the dppe phenyl group and triflate (OTf) counterion compete with one another to bind to the vacant site on the metal center. These weak interactions result in stereochemical rigidity at low temperature. Upon warming, this rigidity breaks down and the ^{31}P NMR peaks sharpen. We also examined the VT NMR spectral behavior of complex **1** without added AB. In this case as well, the spectral properties were similar to those in the reaction of **1** with AB. This rules out any contribution from AB to this dynamic process (see the Supporting Information). Furthermore, Morris and co-workers reported similar downfield shifts of the ^{31}P NMR spectral signals upon cooling for a similar complex $[RuCl(dppe)_2][PF_6]$ alone.[19]

At 198 K, the $^{31}P\{^1H\}$ NMR spectrum showed the presence of the starting material in major quantity. In addition, a very small quantity of **3a** (δ 53.0 ppm), which was evident by the weak intensity of the signal, was also noted. Upon warming to 218 K, three apparent multiplets at δ 79.5, 65.3, and 64.4 ppm for **3b** appeared. Raising the temperature of the reaction mixture further resulted in the evolution of **4**−**6**. Compounds **4** and **5** arise from the binding of H_2 produced from the reaction of $H_3N{\cdot}BH_2Cl$ and AB, which is an intermolecular pathway involving B−H as well as N−H activation in stepwise fashion through on- and off-metal processes, respectively. Dehydrogenation of amine boranes going through on- and off-metal mechanisms has been described in detail recently by Sabo-Etienne et al.[15m] Complexes **4**−**6** adopt a trans geometry with respect to the dppe ligand, making all of the P atoms equivalent to each other; hence, only singlets were noted in the $^{31}P\{^1H\}$ NMR spectrum for these complexes at δ 68.0, 51.5, and 62.3 ppm, respectively.[19,23] Free H_2 generated in the reaction gets consumed by its two major scavengers, complexes **3a**/**3b** and the starting complex **1**, as noted above (Scheme 2, step v). All of these complexes react almost simultaneously with H_2, giving rise to complexes **4** and **5** (Scheme 2, step v). These reactions proceed until all of the H_2 liberated is consumed. The fate of the proton equivalent that results upon heterolysis of the bound H_2 in complex **5** is not known. In order to test whether any of the steps shown in Scheme 2 are reversible, we warmed the sample and recooled it several times. We found no evidence of any of the reactions being reversible. We also carried out the reaction of $[RuCl(dppe)_2][OTf]$ with AB in molar ratios of 1:5 and 1:10. In these experiments, we noted proportionately larger amounts of $H_3N{\cdot}BH_2Cl$ being formed, which ultimately gets

dx.doi.org/10.1021/ic300390s | Inorg. Chem. 2013, 52, 28−36

Scheme 3. Proposed Mechanism of the Reaction of Complex 1 with DMAB[a]

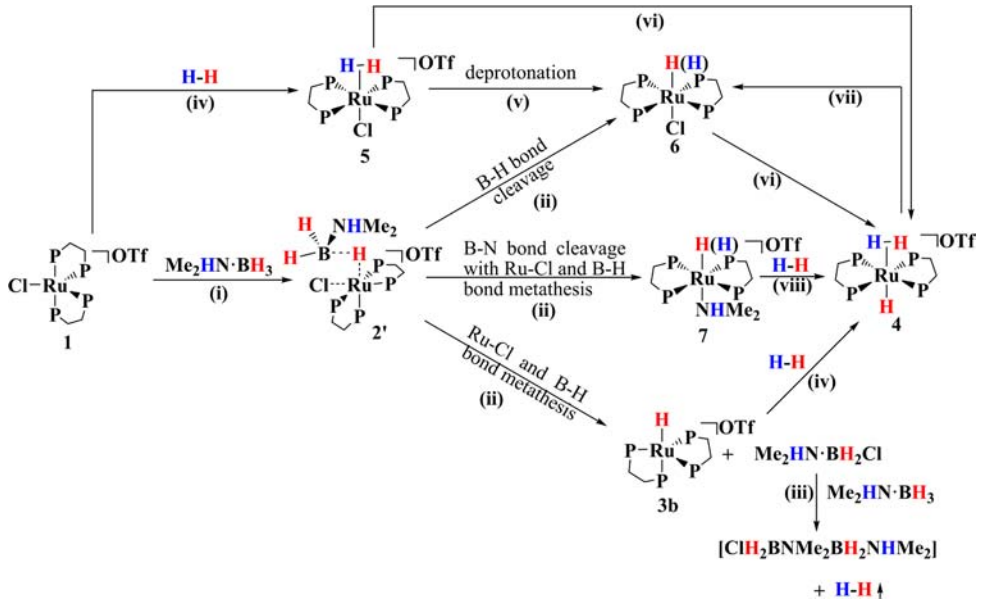

[a]Step vi: transformation of **5** or **6** to **4** takes place in the presence of **6** or **5**, respectively. Step vii: transformation of **4** to **6** takes place in the presence of Cl^-.

transformed into the BNH_x polymer (see the Supporting Information).We also observed the formation of μ-aminodiborane (μ-$NH_2B_2H_5$), which is characterized by a triplet of doublets (1:2:1) signal at δ −26.0 ppm in the ^{11}B NMR spectrum. This species was also established using $^1H-^{11}B$ HETCOR spectroscopy (see the Supporting Information). Stephens et al. provided spectroscopic characterization for μ-aminodiborane as well as the pathway of its formation,[25] and, recently, this compound has also been characterized by X-ray crystallography by Shore et al.[29] The formation of complex **3b** via Ru−Cl and B−H bond metathesis is an example of σ-complex-assisted metathesis (σ-CAM), which has recently been highlighted by Perutz and Sabo-Etienne.[30] The σ-CAM reactions are attracting the interest of organometallic chemists mainly because they could serve as models for metal-complex-catalyzed carbon−heteroatom bond formation in organic synthesis through C−H bond activation.

Herein, the metathesis reaction is facilitated by the affinity of boron toward chlorine as well as having a triflate counterion in complex **1**, which is noncoordinating (or weakly coordinating) in nature, resulting in the formation of a B−Cl rather than a B−OTf bond; $H_3N{\cdot}BH_2Cl$ was noted in the NMR spectra rather than $H_3N{\cdot}BH_2(OTf)$ (see the Supporting Information). In order to establish that B−H bond activation had taken place, we carried out the reaction of complex **1** with $NH_3{\cdot}BD_3$ and noted the formation of HD isotopomers of complex **4**. A triplet featuring a 1:1:1 intensity pattern instead of a broad signal for (Ru-η^2-HD) at δ −4.8 ppm in the ^1H NMR spectrum indicates the presence of isotopomers (see the Supporting Information).[23]

Reaction of Complex 1 with DMAB (1:1). DMAB with two methyl groups on the N atom is sterically encumbered and at the same time possesses an electron-rich B−H bond by virtue of the two methyl substituents. It is slightly less polar than AB and soluble to a greater extent in organic solvents, in particular CH_2Cl_2 rather than AB. The reaction of DMAB with complex **1** at room temperature resulted in the formation of the same products, i.e., **4**−**6**, as in the case of the reaction of AB with complex **1**, and the ^{11}B NMR spectrum showed $Me_2HN{\cdot}BH_2Cl$.[22] Once again in this case we carried out VT NMR spectral measurements to elucidate the reaction pathway (see Scheme 3). The VT NMR spectral studies revealed some interesting features of the reaction, different from those with AB, with a notable one being observation of a σ-borane species as a key intermediate at 193 K. The B−H bond of DMAB approaches the Ru center trans to one of the equatorial P atoms and adjacent to the Cl atom of complex **1**, resulting in a σ-borane intermediate **2′**, wherein the B−H bond bound to the metal is cis to Cl and trans to one of the P atoms of the dppe ligand (Scheme 3, step i). The ^1H NMR spectrum of the reaction mixture at 193 K exhibits a broad singlet at δ −12.1 ppm (Figure 3). We also recorded the $^1H-^1H$ COSY spectrum at 193 K (Figure 4), which revealed that the signal at δ −12.1 ppm correlates with one off-diagonal cross peak at δ ∼1.5 (br) ppm. The integration ratio of these two peaks is ∼1:2, indicating that the high-field signal corresponds to the B−H H atom bound to the metal and the low-field one corresponds to two terminal B−H H atoms in an almost frozen state. Furthermore, the off-diagonal cross peak shows two spots with the center of the contours that are apart by ∼48.0 Hz, suggesting that the B−H bond bound to the metal center is considerably stretched and that it is nearly a hydride. The J(B,H) of 60.0 Hz found for σ-borane complexes by Shimoi et al. has been ascribed to a moderately stretched B−H bond.[12] The $^{31}P\{^1H\}$ NMR spectrum of **2′** is comprised of three signals at δ 39.1 (m), 41.4 (m), and 48.9 (m) ppm, indicating the presence of three kinds of phosphorus environments (Figure 5 and Scheme 3). The broad feature of the spectral signals at 193 K precluded characterization of the σ-borane intermediate **2′** by ^{11}B NMR spectroscopy.

We also measured the spin−lattice relaxation time, T_1, for the ^1H NMR spectral signal at δ −12.1 ppm at 193 K and obtained a value of ∼116 ms, indicating its hydridic nature (see the Supporting Information).[18] The intermediate **2′** undergoes

dx.doi.org/10.1021/ic300390s | Inorg. Chem. 2013, 52, 28−36

three different reactions upon an increase in the temperature of the sample, (a) B−H bond cleavage, (b) Ru−Cl and B−H bond metathesis (via σ-CAM mechanism), and (c) B−N bond cleavage with Ru−Cl and B−H bond metathesis (Scheme 3, step ii), and the evolution of their respective products, **6**, **3b** (trigonal-bipyramidal geometry), and *trans*-[RuH($NHMe_2$)-($dppe)_2$][OTf] (**7**) was noted in the ^{1}H NMR spectrum at 203 K (Figure 3). As in the case of the reaction of complex **1** with AB, we warmed and recooled the sample in the reaction of complex **1** with DMAB several times as well to determine if any of the steps were indeed reversible. We, however, found no evidence that pointed to any of the reactions being reversible. On the other hand, from the data that we have obtained for this reaction, it is not possible for us to decipher whether step ii shown in Scheme 3 proceeds in a stepwise or concerted fashion. Therefore, neither of these pathways can be ruled out. Compound **6** is also formed via the intermediacy of **5**, which undergoes heterolytic cleavage of the bound H_2 ligand. The origin of **5** is the reaction of the starting complex **1** with H_2. The relatively unstable **3b** picks up H_2 produced from the reaction of $Me_2HN{\cdot}BH_2Cl$ or $Me_2HN{\cdot}BH_2(OTf)$ (see the Supporting Information) and the unreacted DMAB to form **4**, which was also noted in the ^{1}H NMR spectrum at 203 K. Upon an increase in the sample temperature, the concentration of **4** builds up at the expense of **3b** (Figures 3 and 5). On the other hand, Ru−Cl and B−H bond metathesis with concerted B−N bond cleavage (Scheme 3, step ii) leads to the formation of cationic complex **7**, which exhibits a quintet at δ −17.3 ppm and a singlet at δ 65.0 ppm in the ^{1}H and ^{31}P{^{1}H} NMR spectra, respectively. This species is stable up to a temperature of 253 K, above which it almost completely transforms to **4** (see Figure 3). On the basis of the ^{31}P{^{1}H} inversion−recovery experiment (see the Supporting Information) on the reaction mixture at 203 K, we noted that **4** and **7** interconvert by slow reaction rates.

Recently, Whittlesey and co-workers observed the σ-borane complex [Ru(xantphos)(PPh_3)($H_3B{\cdot}NH_3$)H)][$BAr^F{}_4$] [xantphos = 4,5-bis(diphenylphosphino)-9,9′-dimethylxanthene; $BAr^F{}_4$ = [B{3,5-$(CF_3)_2C_6H_3$}$_4$]$^-$] in the reaction of [Ru(xantphos)(PPh_3)(OH_2)H)][$BAr^F{}_4$] with AB in which AB coordinates through the B−H bond to ruthenium. After 72 h, they found a mixture of complexes [Ru(xantphos)(PPh_3)(η^2-H_2)H)][$BAr^F{}_4$] and [Ru(xantphos)(PPh_3)(NH_3)H)][$BAr^F{}_4$]. The latter species forms when the σ-borane complex undergoes B−N bond cleavage assisted by H_2O in the dehydrogenation process of AB followed by the coordination of NH_3 to ruthenium.[31] In an independent reaction of complex **1** and AB having a mixture of complexes **4** and **6**, with aqueous NH_3, a quintet at δ −17.3 ppm was noted in the ^{1}H NMR spectrum, indicating the formation of *trans*-[RuH(NH_3)($dppe)_2$][OTf] as the exclusive product. In a separate reaction of complex **4** with AB, again *trans*-[RuH(NH_3)($dppe)_2$][OTf] was obtained as the sole product (for details, see the Supporting Information). The VT ^{11}B NMR spectral stack plot revealed the presence of $Me_2HN{\cdot}BH_2(OTf)$, whose intensity fades upon an increase in the sample temperature with the concomitant evolution of $Me_2HN{\cdot}BH_2Cl$ (Figure 6). As in the case of the reaction of **1** with AB, the species that persist upon warming the sample to room temperature in the reaction of **1** with DMAB are **4**−**6**. The VT ^{31}P{^{1}H} NMR spectral studies are in conformity with those of ^{1}H NMR spectral studies. Spectral signals were noted for the σ-borane intermediate (**2′**) at 193 K, three signals at δ 39.1 (m), 41.4 (m), and 48.9 (m) ppm, indicating the presence

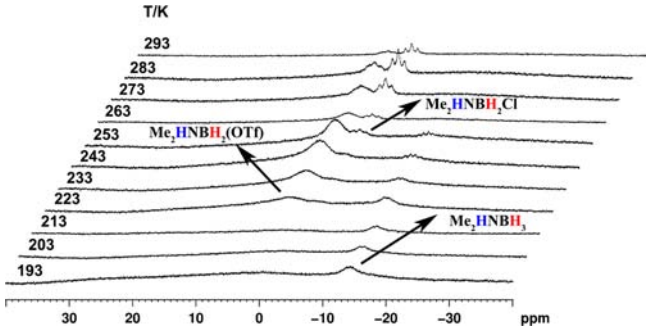

Figure 6. ^{11}B NMR spectral stack plot with temperature showing $Me_2HN{\cdot}BH_2(OTf)$ and $Me_2HN{\cdot}BH_2Cl$ in the reaction of complex **1** with DMAB in CD_2Cl_2.

of three kinds of phosphorus environments, whereas those of complexes **4**−**6** along with the intermediate **3b** appeared when the temperature was raised (Figure 5 and Scheme 3). Surprisingly, in this case, we did not observe complex **3a** in the ^{1}H NMR as well as in the ^{31}P{^{1}H} NMR spectra. We attempted to characterize **2′** further by ^{1}H−^{31}P correlation spectroscopy at 193 K. However, no correlation spot was found, which could be due to the low concentration of the intermediate **2′** in the solution (see the Supporting Information).

Reaction of 1 with Excess AB and DMAB. Reaction of complex **1** with excess AB and DMAB were performed at both room and variable temperature. The reaction in each case proceeded with vigorous gas evolution and resulted in species that were similar to those obtained in the stoichiometric (1:1) reactions and were identified and characterized; in addition, the reactions, however, were rendered complex by the formation of multiple species, which could not be identified and unambiguously characterized. The reaction of complex **1** with excess AB at room temperature afforded complexes **4**, **6**, and *trans*-[RuH(NH_3)($dppe)_2$][OTf] and an unidentified species based on ^{1}H and ^{31}P{^{1}H} NMR spectroscopy (see the Supporting Information). However, the ^{11}B NMR spectrum at room temperature revealed the presence of the BNH_x polymer, μ-aminodiborane, and $H_3N{\cdot}BH_2Cl$ (see the Supporting Information).

We also carried out a VT NMR (^{1}H, ^{31}P{^{1}H}, and ^{11}B) spectral study of the reaction of complex **1** with excess AB. In this reaction, we noted the evolution of complexes **4**−**6** and *trans*-[RuH(NH_3)($dppe)_2$][OTf] through the intermediacy of **3a** and **3b**. The spectral features of the *trans*-[RuH(NH_3)-($dppe)_2$][OTf] complex obtained as part of this mixture matched those of an independently prepared sample (see the Supporting Information). In addition, an unidentified species that shows a broad peak at δ −2.6 ppm in the ^{1}H NMR spectrum was also noted. This signal appeared at 293 K. The ^{31}P{^{1}H} NMR spectrum corroborates with the ^{1}H NMR spectral features with regard to the formation of complexes **4**−**6** and *trans*-[RuH(NH_3)($dppe)_2$][OTf]. The ^{11}B NMR spectra, however, showed the presence of $H_3N{\cdot}BH_2Cl$[21] and another unidentified species.

On the other hand, complex **1** reacts with excess DMAB at room temperature to give complexes **4** and **6** and some other unidentified species, as evidenced by ^{1}H and ^{31}P{^{1}H} NMR spectroscopy (Supporting Information). The ^{11}B NMR spectrum showed the presence of the cyclic dimer $(Me_2NBH_2)_2$,[15a,32] showing a triplet at δ ∼5.0 ppm [J(B,H)

dx.doi.org/10.1021/ic300390s | Inorg. Chem. 2013, 52, 28−36

≈ 112 Hz], a broad triplet of doublets (1:2:1) at δ −17.8 ppm assignable to μ-aminodiborane ($H_2B(\mu\text{-}H,NMe_2)BH_2$),[33] a triplet at δ ∼37 ppm corresponding to $H_2B{=}NMe_2$,[32d] and a few other unknown species. Cyclic dimer $(Me_2NBH_2)_2$ formation could be an off-metal as well as an on-metal process.[15m] The VT ^1H and $^{31}P\{^1H\}$ NMR spectral stack plots of the reaction of complex **1** with excess DMAB revealed the presence of complexes **2′**, **3b**, **4**, **6**, and **7**. The VT ^{11}B NMR spectral stack plot showed the formation of $Me_2HN{\cdot}BH_2(OTf)$ at 223 K, and as the temperature of the sample was raised, $Me_2HN{\cdot}BH_2Cl$[22] was also noted. The spectral assignment of $Me_2HN{\cdot}BH_2(OTf)$ was confirmed using a sample prepared independently by reacting DMAB and HOTf (see the Supporting Information).

Thus, reactions of complex **1** with excess AB and DMAB gave rise to products that were common to those of reactions with stoichiometric amounts. At the same time, few other products were also formed that could not be definitively characterized, as a result of which the mechanistic pathways in these cases could not be deduced.

CONCLUSIONS

The ruthenium complex $[RuCl(dppe)_2][OTf]$ brings about B−H bond activation and cleavage in AB and DMAB via the intermediacy of $[RuCl(\eta^1\text{-}HBH_2{\cdot}NH_3)(dppe)_2][OTf]$ and $[RuCl(\eta^1\text{-}HBH_2{\cdot}NMe_2H)(dppe)_2][OTf]$, respectively. Because the ruthenium complex **1** was found to be quite reactive toward AB and DMAB, multinuclear VT NMR spectral studies were carried out to decipher the various intermediate species that were formed enroute to the final products. On the basis of these studies, the reaction pathway in each case was deduced and proposed.

ASSOCIATED CONTENT

Supporting Information

NMR spectral data of the reactions and spin−lattice relaxation time (T_1, ms) measurements data. This material is available free of charge via the Internet at http://pubs.acs.org.

AUTHOR INFORMATION

Corresponding Author

*E-mail: jagirdar@ipc.iisc.ernet.in.

Notes

The authors declare no competing financial interest.

ACKNOWLEDGMENTS

We are grateful to the Department of Science & Technology, India (Science & Engineering Research Board, India), for financial support.

REFERENCES

(1) Labinger, J. A.; Bercaw, J. E. *Nature* **2002**, *417*, 507.
(2) Kubas, G. J. *Chem. Rev.* **2007**, *107*, 4152.
(3) Kubas, G. J. *Metal Dihydrogen and Sigma-Bond Complexes: Structure, Theory, and Reactivity*; Kluwer Academic: New York, 2001.
(4) Kubas, G. J. *Adv. Inorg. Chem.* **2004**, *56*, 127.
(5) Sabo-Etienne, S.; Chaudret, B. *Coord. Chem. Rev.* **2008**, *252*, 2395.
(6) Corey, J. Y. *Chem. Rev.* **2011**, *111*, 863.
(7) Hall, C.; Perutz, R. N. *Chem. Rev.* **1996**, *96*, 3125.
(8) Bercaw, J. E.; Labinger, J. A. *Proc. Natl. Acad. Sci. U.S.A.* **2007**, *104*, 6899.
(9) Cowan, A. J.; George, M. W. *Coord. Chem. Rev.* **2008**, *252*, 2504.
(10) Bernskoetter, W. H.; Schauer, C. K.; Goldberg, K. I.; Brookhart, M. *Science* **2009**, *326*, 553.
(11) Hartwig, J. F.; Muhoro, C. N.; He, X.; Eisenstein, O.; Bosque, R.; Maseras, F. *J. Am. Chem. Soc.* **1996**, *118*, 10936.
(12) Shimoi, M.; Nagai, S.; Ichikawa, M.; Kawano, Y.; Katoh, K.; Uruichi, M.; Ogino, H. *J. Am. Chem. Soc.* **1999**, *121*, 11704.
(13) Alcaraz, G.; Sabo-Etienne, S. *Angew. Chem., Int. Ed.* **2010**, *49*, 7170.
(14) Staubitz, A.; Robertson, A. P. M.; Manners, I. *Chem. Rev.* **2010**, *110*, 4079.
(15) (a) Jaska, C. A.; Temple, K.; Lough, A. J.; Manners, I. *J. Am. Chem. Soc.* **2003**, *125*, 9424. (b) Jaska, C. A.; Manners, I. *J. Am. Chem. Soc.* **2004**, *126*, 1334. (c) Shrestha, R. P.; Diyabalanage, H. V. K.; Semelsberger, T. A.; Ott, K. C.; Burrell, A. K. *Int. J. Hydrogen Energy* **2009**, *34*, 2616. (d) Denney, M. C.; Pons, V.; Hebden, T. J.; Heinekey, D. M.; Goldberg, K. I. *J. Am. Chem. Soc.* **2006**, *128*, 12048. (e) Blaquiere, N.; Diallo-Garcia, S.; Gorelsky, S. I.; Black, D. A.; Fagnou, K. *J. Am. Chem. Soc.* **2008**, *130*, 14034. (f) Käß, M.; Friedrich, A.; Drees, M.; Schneider, S. *Angew. Chem., Int. Ed.* **2009**, *48*, 905. (g) Keaton, R. J.; Blacquiere, J. M.; Baker, R. T. *J. Am. Chem. Soc.* **2007**, *129*, 1844. (h) Conley, B. L.; Williams, T. J. *Chem. Commun.* **2010**, *46*, 4815. (i) Chapman, A. M.; Haddow, M. F.; Wass, D. F. *J. Am. Chem. Soc.* **2011**, *133*, 8826. (j) Wright, W. R. H.; Berkeley, E. R.; Alden, L. R.; Baker, R. T.; Sneddon, L. G. *Chem. Commun.* **2011**, *47*, 3177. (k) Kim, S.-K.; Han, W.-S.; Kim, T.-J.; Kim, T.-Y.; Nam, S. W.; Mitoraj, M.; Pieko, L.; Michalak, A.; Hwang, S.-J.; Kang, S. O. *J. Am. Chem. Soc.* **2010**, *132*, 9954. (l) Conley, B. L.; Guess, D.; Williams, T. J. *J. Am. Chem. Soc.* **2011**, *133*, 14212. (m) Stevens, C. J.; Dallanegra, R.; Chaplin, A. B.; Weller, A. S.; Macgregor, S. A.; Ward, B.; McKay, D.; Alcaraz, G.; Sabo-Etienne, S. *Chem.—Eur. J.* **2011**, *17*, 3011. (n) Chaplin, A. B.; Weller, A. S. *Inorg. Chem.* **2010**, *49*, 1111. (o) Chaplin, A. B.; Weller, A. S. *Angew. Chem., Int. Ed.* **2010**, *49*, 581. (p) Johnson, H. C.; Robertson, A. P. M.; Chaplin, A. B.; Sewell, L. J.; Thompson, A. L.; Haddow, M. F.; Manners, I.; Weller, A. S. *J. Am. Chem. Soc.* **2011**, *133*, 11076. (q) Douglas, T. M.; Chaplin, A. B.; Weller, A. S. *J. Am. Chem. Soc.* **2008**, *130*, 14432. (r) Sewell, L. J.; Lloyd Jones, G. C.; Weller, A. S. *J. Am. Chem. Soc.* **2012**, *134*, 3598. (s) Alcaraz, G.; Vendier, L.; Colt, E.; Sabo-Etienne, S. *Angew. Chem., Int. Ed.* **2010**, *49*, 918. (t) Paul, A.; Musgrave, C. B. *Angew. Chem., Int. Ed.* **2007**, *46*, 8153.
(16) Ramachandran, P. V.; Gagare, P. D. *Inorg. Chem.* **2007**, *46*, 7810.
(17) Fox, A. M.; Harris, E. J.; Heider, S.; Pérez-Gregorio, V.; Zakrzewska, E. M.; Farmer, D. J.; Yufit, D. S.; Howard, J. A. K.; Low, P. J. *J. Organomet. Chem.* **2009**, *694*, 2350.
(18) Hamilton, D. G.; Crabtree, R. H. *J. Am. Chem. Soc.* **1988**, *110*, 4126.
(19) Chin, B.; Lough, A. J.; Morris, R. H.; Schweitzer, C. T.; D'Agostino, C. *Inorg. Chem.* **1994**, *33*, 6278.
(20) Nishibayashi, Y.; Takei, I.; Hidai, M. *Angew. Chem., Int. Ed.* **1999**, *38*, 3047.
(21) Hu, M. G.; Geanangel, R. A. *Inorg. Chem.* **1979**, *12*, 3297.
(22) Nöth, H.; Bayer, H. *Chem. Ber.* **1960**, *93*, 2251.
(23) Bautista, M. T.; Cappellani, E. P.; Drouin, S. D.; Morris, R. H.; Schweitzer, C. T.; Sella, A.; Zubkowski, J. *J. Am. Chem. Soc.* **1991**, *113*, 4876.
(24) Jasim, N. A.; Perutz, R. N.; Foxon, S. P.; Walton, P. H. *J. Chem. Soc., Dalton Trans.* **2001**, 1676.
(25) Stephens, F. H.; Baker, R. T.; Matus, M. H.; Grant, D. J.; Dixon, D. A. *Angew. Chem., Int. Ed.* **2007**, *46*, 746.
(26) Stephens, F. H.; Pons, V.; Baker, R. T. *Dalton Trans.* **2007**, 2613.
(27) Atkins, P.; De Paula, J. *Atkins' Physical Chemistry*, 8th ed.; Oxford University Press: Oxford, U.K., 2006.
(28) Mezzetti, A.; Zotto, A. D.; Rigo, P. *J. Chem. Soc., Dalton Trans.* **1989**, 1045.
(29) Chen, X.; Zhao, J.; Shore, S. G. *J. Am. Chem. Soc.* **2010**, *132*, 10658.
(30) Perutz, R. N.; Sabo-Etienne, S. *Angew. Chem., Int. Ed.* **2007**, *46*, 2578.

(31) Ledger, A. E. W.; Ellul, C. E.; Mahon, M. F.; Williams, J. M. J.; Whittlesey, M. K. *Chem.—Eur. J.* **2011**, *17*, 8704.
(32) (a) Jaska, C. A.; Temple, K.; Lough, A. J.; Manners, I. *Chem. Commun.* **2001**, 962. (b) Burg, A. B.; Randolph, C. L., Jr. *J. Am. Chem. Soc.* **1949**, *71*, 3451. (c) Haubold, W.; Schaeffer, R. *Chem. Ber.* **1971**, *104*, 513. (d) Nöth, H.; Vahrenkamp, H. *Chem. Ber.* **1967**, *100*, 3353.
(33) Phillips, W. D.; Miller, H. C.; Muetterties, E. L. *J. Am. Chem. Soc.* **1959**, *81*, 4496.